Influence of electric field on a first-order smectic-A–ferroelectric-smectic-C liquid-crystal phase transition: A field-induced critical point

Ch. Bahr and G. Heppke
Iwan-N.-Stranski-Institute for Physical and Theoretical Chemistry, Technical University of Berlin, D-1000 Berlin 12, Federal Republic of Germany
(Received 4 December 1989)

The observation of a new critical point in liquid-crystal phase transitions is reported. Detailed tilt-angle, polarization, and susceptibility measurements of a ferroelectric liquid-crystal compound in the presence of an applied dc electric field show that a first-order phase transition between the polarized smectic-A phase and the ferroelectric-smectic-C phase terminates at a critical point in the temperature field plane. A liquid-crystal sample exhibiting a second-order smectic-A–ferroelectric-smectic-C transition is studied by similar measurements demonstrating a clearly different behavior to the first-order compound. A simple Landau description of the new critical point is given.

I. INTRODUCTION

Smectic-A (Sm-A) and smectic-C (Sm-C) liquid-crystal phases are orientationally ordered fluids with a one-dimensional density wave, the wave vector being either parallel (Sm-A) or tilted (Sm-C) with respect to the director (i.e., the average direction of the long molecular axis). Such a structure may also be considered as an arrangement of the rodlike molecules in weakly defined layers with the molecules oriented on average parallel (Sm-A) to the normal vector of the layers or at a tilt angle θ to the layer normal (Sm-C). Many liquid-crystal compounds exhibit both the Sm-A and the Sm-C phase, the latter being the low-temperature phase.

Considerable effort has been spent[1] studying Sm-A and Sm-C phases composed of chiral (i.e., without mirror plane) molecules, because of their ferroelectric and quasi-piezoelectrical properties based on a coupling between tilt angle and electric polarization. In 1975 Meyer *et al.*[2] showed that, if the constituent molecules are chiral and possess a permanent transverse dipole, each layer of the Sm-C phase exhibits a spontaneous polarization, the polarization vector pointing parallel to the smectic layer plane and perpendicular to the tilted director. As a second consequence of the molecular chirality the director builds up a helical superstructure by precessing around the layer normal. The corresponding helical pitch amounts to usually several μm, the molecular short-range order being the same as in the nonchiral Sm-C phase. A dc electric field of sufficient strength unwinds the helical structure by aligning the polarization vectors of the smectic layers parallel to the field direction, thus producing a homogeneous orientation of the director.

The coupling between tilt and polarization, which causes the spontaneous polarization in the Sm-C phase of chiral molecules, can also be observed in the high-temperature Sm-A phase as the so-called electroclinic effect,[3] a kind of inverse piezoelectric effect. The director in the Sm-A phase, usually being parallel to the layer normal, becomes tilted when a dc electric field is applied parallel to the layer plane. The direction of the induced tilt is perpendicular to the field direction and the magnitude proportional to the applied field strength. Both the ferroelectricity in the Sm-C phase and the electroclinic effect in the Sm-A phase possess considerable technological potential because they enable electro-optic effects in the microsecond and submicrosecond range.

The phase transition between Sm-A and Sm-C is generally second order, i.e., the tilt angle, which can be taken as the primary order parameter of the transition, decreases continuously to zero when approaching the transition from the low-temperature side. Although it was initially proposed[4] that the transition might exhibit helium-like critical behavior, subsequent studies[5–12] have shown that the transition is mean-fieldlike with an unusually large sixth-order term in the Landau free-energy expansion.

Recently, the first experimental examples for a discontinuous first-order Sm-A–Sm-C transition were observed in some chiral (and thus ferroelectric) compounds exhibiting large values of the spontaneous polarization.[13] In principle, the basic properties of the Sm-A–ferroelectric-Sm-C transition in chiral compounds are expected to be the same as in nonchiral compounds because in the ferroelectric case the transition is driven also by molecular interactions producing the tilt and not by interactions between permanent dipoles.[10,14] Consequently, the Sm-A–ferroelectric-Sm-C transition is in most cases second order and shows the same critical behavior as the nonferroelectric transition. The origin of the first-order behavior in some ferroelectric compounds is still the subject of current research[15] and the actual reason for the occurrence of a discontinuous Sm-A–Sm-C transition is not clarified. However, the availability of ferroelectric liquid-crystal compounds showing a first-order Sm-A–Sm-C transition enables the investigation of new phenomena such as the electric-field-induced critical point on which we report in this study.

As described above, in the presence of a dc electric field applied parallel to the smectic layers Sm-A and Sm-

C phase show a tilt angle with the same homogeneous tilt direction (if the field is sufficient to unwind the helical structure of the Sm-C phase). Then, the Sm-A and the Sm-C phase have identical symmetry and are thermodynamically distinct only if a first-order transition exists at which the tilt angle shows a discontinuous behavior. We present here the first detailed experimental study of such a first-order Sm-A–ferroelectric-Sm-C transition in the presence of an electric field (preliminary results of our study were reported as a Rapid Communication[16]). Measurements of tilt angle, polarization, and susceptibility as function of temperature and field strength show that the first-order transition, characterized by a discontinuity of tilt angle and polarization, vanishes when the field strength exceeds a critical value. The results establish a new type of critical point in liquid-crystal phase transitions. By adding a small amount of a second liquid-crystal compound to our initial sample, the first-order Sm-A–Sm-C transition was driven to become second order. The different behavior of this second-order transition is demonstrated by additional measurements of the electric field dependence of tilt angle and susceptibility. Finally, we give a simple mean-field description of the critical point by means of Landau theory.

II. EXPERIMENT

We have studied two liquid-crystal samples. Most of the measurements are carried out for the chiral compound (S,S)-4-(3-methyl-2-chloropentanoyloxy)-4'-heptylozybiphenyl (abbreviated as C7, the structural formula is shown on the top of Fig. 4). This compound is the first experimental example for a first-order Sm-A–ferroelectric-Sm-C transition.[13] The phase sequence and the transition temperatures of the C7 liquid crystal are Sm-G 44 °C Sm-C 55.0 °C Sm-A 62 °C isotropic. (Sm-G denotes a more-ordered smectic phase possessing, in contrast to Sm-A and Sm-C, a three-dimensional long-range positional order of the molecules.) The second sample consists of a binary mixture of C7 with the compound 4-butyloxyphenyl-4'-decyloxybenzoate (abbreviated as 10.0.4). The composition of the mixture is 80 wt % of C7+20 wt % of 10.0.4 and its transition temperatures are Sm-C 45.6 °C Sm-A 60 °C isotropic. As described below, the Sm-A–Sm-C transition of this mixture is second order.

A. Sample preparation

The sample in its isotropic phase is loaded into a conductively coated glass cell (thickness 10 μm, electrode area 16 mm^2). The glass surface is coated with a rubbed polymer layer in order to give a planar alignment of the liquid-crystal molecules. The cell is placed into an oven consisting of a copper block heated by a water thermostat (Haake F3). The oven, provided with a good thermal insulation, allows for optical observation of the sample. The temperature, measured by a 100-kΩ thermistor, is kept stable within 10 mK or is changed at a constant rate of 10 mK/min. A homogeneous planar alignment of the liquid crystal is achieved by slow cooling of the sample from the isotropic phase to the Sm-A phase with a moderate ac electric field applied (1 kHz, 40 V). All measurements described below are carried out in this sample configuration (i.e., the director and the smectic layer normal of the liquid crystal are parallel to the glass surface, the electric field is applied parallel to the smectic layer planes). We should note that, for our relatively thick sample with a dc electric field applied, we do not see an indication of the so-called chevron structure,[17] i.e., a tilt of the smectic layers with respect to the glass surface occurring in thin Sm-C samples.

B. Tilt-angle measurement

The field-induced tilt angle in the Sm-A phase is determined optically by measuring the switching angle between the director positions at positive and negative applied dc electric field. The computer-controlled setup is shown schematically in Fig. 1. The sample is placed under a polarizing microscope between two crossed polarizers which can be simultaneously rotated by a step motor. The intensity of transmitted light varies as $\sin^2(2\varphi)$ where φ denotes the angle between director and plane of polarization. A square wave field with the frequency of 1 Hz is applied, the director is then switching by twice the amount of the induced tilt angle changing the angle φ by the same amount. During each switching period the polarizers are rotated by 1° while the intensity of transmitted light is measured by a photomultiplier for positive and negative applied field. Thus we obtain two curves of light intensity versus angular position of the polarizers (Fig. 2). The phase shift between the curves, which can be determined with an accuracy better than 0.1°, corresponds to twice the amount of the induced tilt angle. By the same method the switching angle in the Sm-C phase, consisting of the sum of intrinsic tilt angle and field-

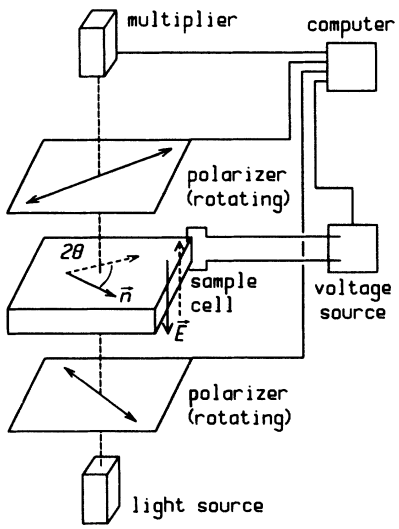

FIG. 1. Experimental setup for the tilt-angle measurements. The two positions of the director n are shown corresponding to the up and down state of the field E. The computer reads the light intensity value from the multiplier, reverses the applied dc field, and reads the light intensity again. Then, the crossed polarizers are rotated by 1° and the procedure starts again until the polarizers are rotated by 90°. The multiplier is mounted at the top of a microscope (not shown in the figure) and the sample can be observed by the eye simultaneous to the measurements.

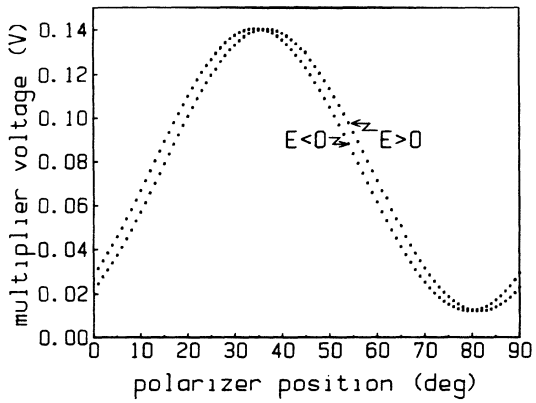

FIG. 2. Typical experimental curves of light intensity (multiplier voltage) vs angular position of the crossed polarizers. The phase shift is equal to the switching angle between director positions at positive and negative applied field.

induced tilt angle, can be measured if the field is sufficient to unwind the helix. The unwinding field strengths are 5–10 kV/cm for pure C7 and 1–2 kV/cm for the second-order mixture: all measurements reported in this paper are for unwound samples.

C. Polarization measurement

The polarization is determined by the field reversal method.[18] A square wave field of 1 Hz is applied to the cell while the current through a resistor in series with the cell is monitored on a digital storage oscilloscope. The current versus time curves in the Sm-C phase consist of a sharp peak occurring immediately after field reversal—corresponding to the reversal of induced polarization—and a second broad peak corresponding to the reversal of the spontaneous polarization. In the Sm-A phase only the first peak is obtained. The integral of the current versus time curve corresponds to the electric displacement (i.e., spontaneous polarization plus induced polarization plus $\epsilon_0 E$) of the sample in the applied field. Typical experimental curves are shown in Fig. 3. The measurements are carried out either at constant temperature while the amplitude of the square wave field is changed by a motor-potentiometer at a slow constant rate (10 kV/cm/h) or at constant field amplitude and slowly changing temperature (rate 10 mK/min). The current

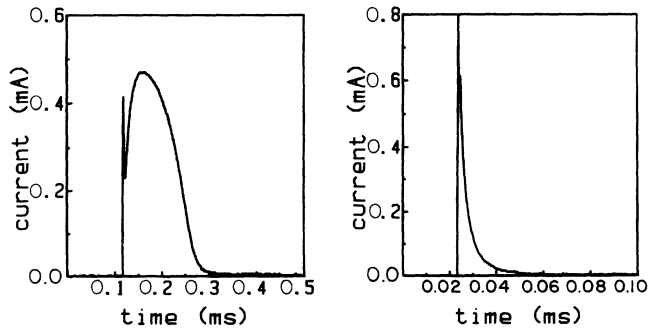

FIG. 3. Typical experimental curves of the polarization reversal current vs time in the Sm-C (left) and Sm-A phase (right).

versus time curves are transferred from the oscilloscope to a computer which calculates the values of the electric displacement.

D. Susceptibility measurement

Measurements of the static electric susceptibility are carried out by determining the capacitance of the sample cell using a HP 4274A *LCR* meter. The capacitance is measured at a frequency of 100 Hz with a measuring voltage of 0.1 V_{rms}. The *LCR* meter allows for the application of a dc bias voltage up to 200 V from an external source. The bias field is reversed with a frequency of 1 Hz in order to avoid electrochemical decomposition of the sample. The measurements are carried out at slowly changing temperature (rate 10 mK/min) while capacitance values are collected continuously by the computer connected to the *LCR* meter. The dielectric constant is calculated by dividing by the capacitance of the empty cell.

III. RESULTS

Figure 4 shows the tilt angle θ determined as a function of the applied dc field E at various temperatures near the zero-field Sm-A–Sm-C transition temperature T_{c_0} (55.0 °C). At temperatures 2 K and more above T_{c_0} we find a simple proportionality between θ and E, i.e., the usual electroclinic behavior of the field-induced tilt in the Sm-A phase (curves a and b). When the temperature is closer to T_{c_0}, the θ versus E curves deviate from the pure linear behavior and become S like in shape exhibiting a nonlinear increase (curves c, d, and e). On further approaching T_{c_0}, the nonlinear increase becomes more pronounced and shifts to lower field strength (curves f, g, h,

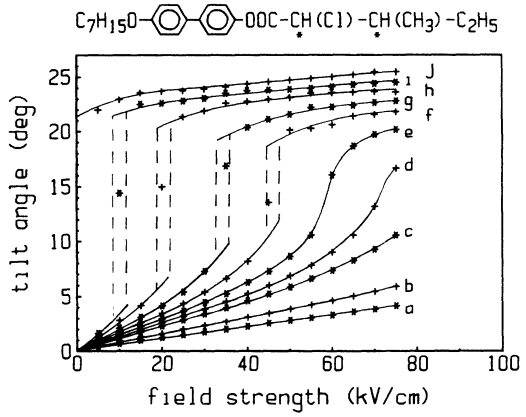

FIG. 4. Electric field dependence of the tilt angle of C7 (structural formula on top of the figure) at various temperatures near the zero-field transition temperature T_{c_0}. The differences to T_{c_0} are (in K) curve a, +3.1; curve b, +2.1; curve c, +1.3; curve d, +1.1; curve e, +0.9; curve f, +0.7; curve g, +0.5; curve h, +0.3; curve i, +0.1; curve j −0.1. Solid lines are only guides to the eye, dashed lines indicate optically observed two-phase regions.

and *i*). Below T_{c_0}, θ is again almost linearly related to E (curve *j*) and one can determine the intrinsic tilt in the Sm-*C* phase by extrapolating the θ values to zero field.

For the curves *f*, *g*, *h*, and *i* in Fig. 4 we observe in the microscope the occurrence of a two-phase region: when the field approaches the values indicated by the dashed lines in Fig. 4, the homogeneous Sm-*A* texture becomes interspersed with small islands characterized by a different birefringence color and surrounded by a sharp phase boundary. When crossing the two-phase region, these islands grow and fuse leaving small islands of the initial texture that finally disappear. The new (Sm-*C*) texture is again homogeneous and differs from the initial (Sm-*A*) texture only by the birefringence color. The two-phase region is observed at the temperature 0.1, 0.3, 0.5, and 0.7 K above T_{c_0} but is not observed for temperatures 0.9 K and more above T_{c_0} where a continuous change of the texture color occurs.

The same behavior as demonstrated by the tilt-angle measurements described above is expected for the polarization of our sample. While for the measurement of one tilt angle data-point temperature and field amplitude must be kept constant for some minutes, the measurements of the polarization can be carried out continuously with the field amplitude or the temperature changing at a slow constant rate as described in the experimental section. The results are shown in Figs. 5 and 6 where the electric displacement D of our sample is plotted either as a function of field strength at constant temperature or as a function of temperature at constant field. At field strengths up to 50 kV/cm and temperatures up to 0.8 K above T_{c_0} the *D*-*E* and *D*-*T* curves exhibit a pronounced increase or drop of the D values shifting to higher temperatures with increasing field. The increase or drop of the D values is accompanied by the optically observable two-phase region described above. In addition, a hysteresis is seen between runs with increasing and decreasing field or temperature. Both two-phase region and hysteresis indicate that the *D*-*E* and *D*-*T* curves display a first-order transition characterized by a discontinuous jump of D. The discontinuity of D, which in the ideal case should occur at a sharp field and temperature value, is in reality spread over a finite field and temperature interval (≈ 5 kV/cm and ≈ 0.1 K, respectively) because of experimental imperfections such as sample impurities and gradients in field strength (sample thickness) and temperature. Two-phase region and hysteresis are not observable when field strength and temperature are above 50 kV/cm and 55.8 °C ($T_{c_0}+0.8$ K) and the *D*-*E* and *D*-*T* curves exhibit a continuous variation of D with E and T.

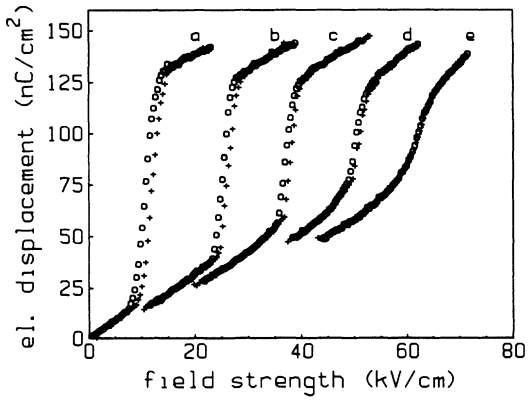

FIG. 5. Electric field dependence of the electric displacement of C7 at various temperatures near T_{c_0}. The differences to T_{c_0} are (in K) curve *a*, +0.2; curve *b*, +0.4; curve *c*, +0.6; curve *d*, +0.8; curve *e*, 1.0; + symbols denote runs with increasing field, ○ symbols denote runs with decreasing field.

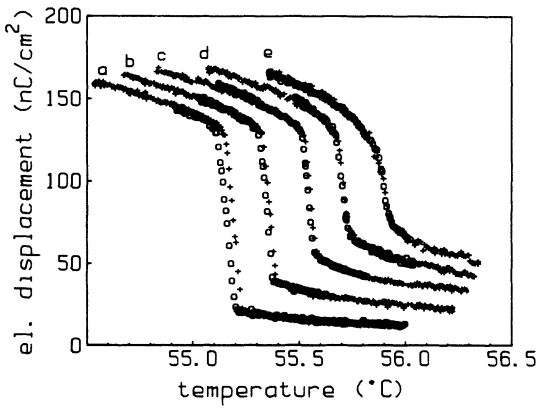

FIG. 6. Temperature dependence of the electric displacement of C7 at various dc field strengths E. The values of E are (in kV/cm) curve *a*, 10; curve *b*, 20; curve *c*, 30; curve *d*, 40; curve *e*, 50; + symbols denote runs with increasing temperature, ○ symbols denote runs with decreasing temperature.

The data presented in Figs. 4–6 show that the C7 liquid crystal in the presence of a low dc electric field exhibits a first-order transition characterized by a discontinuous jump of tilt angle and polarization. With increasing field strength the transition temperature shifts to higher values while the discontinuity becomes less pronounced. At fields larger than about 50 kV/cm there is no first-order transition, but a continuous evolution from the polarized Sm-*A* to the ferroelectric Sm-*C* phase exists. Thus the overall experimental behavior of the ferroelectric liquid crystal is very similar to that of a liquid near the liquid-gas critical point, tilt angle and electric field strength corresponding to density and pressure, respectively. A rough estimation of the critical-point coordinates of our C7 sample gives $T_c \approx 55.8$ °C (i.e., 0.8 K above T_{c_0}), $E_c \approx 50$ kV/cm, and $D_c \approx 100$ nC/cm^2.

As the compressibility diverges at a liquid-gas critical point, the tilt susceptibility $d\theta/dE$ and the differential permittivity dD/dE of the ferroelectric liquid crystal should diverge at the Sm-*A*–Sm-*C* critical point. Figure 7 shows the temperature dependence of the static dielectric constant of our sample at various dc bias fields. Whereas at field strengths of 10 and 30 kV/cm (curves *a* and *b*) the dielectric constant shows a steplike discontinuity corresponding to the first-order transition, a relatively sharp maximum is observed for 50 kV/cm (curve *c*) which becomes lower and broadens when the bias field is increased further up to 70 kV/cm (curve *d*). The temper-

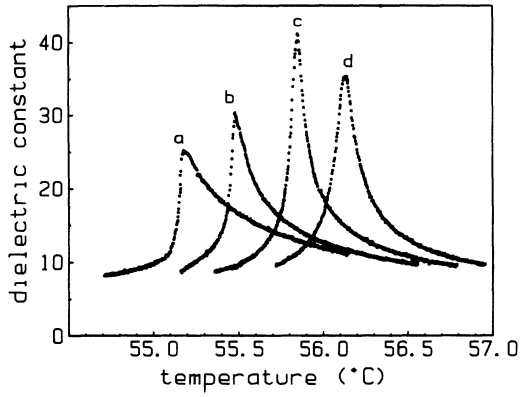

FIG. 7. Temperature dependence of the static dielectric constant of C7 at various bias field strengths. The values of the bias field are (in kV/cm) curve *a*, 10; curve *b*, 30; curve *c*, 50; curve *d*, 70.

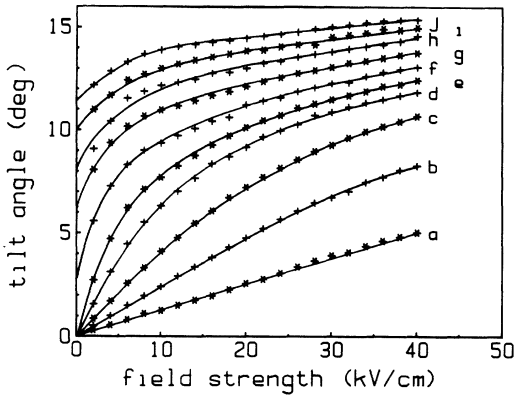

FIG. 8. Electric field dependence of the tilt angle of the second-order mixture at various temperatures near the Sm-*A*–Sm-*C* transition temperature T_c. The differences to T_c are (in K) curve *a*, +2.1; curve *b*, +1.1; curve *c*, +0.6; curve *d*, +0.3; curve *e*, +0.1; curve *f*, −0.1; curve *g*, −0.3; curve *h*, −0.5; curve *i* −0.7; curve *j*, −0.9. Solid lines are only guides to the eye.

ature dependence of the dielectric constant at a bias field of 50 kV/cm might indicate the expected divergencelike behavior although the rounding of our data due to experimental imperfections does not allow for a definite conclusion.

The same behavior as described above for the ferroelectric liquid crystal is found also for solid-state ferroelectrics such as potassium dihydrogen phosphate (KDP).[19,20] The first-order paraelectric-ferroelectric transition of KDP vanishes at a critical field of ≈ 0.2 kV/cm at a temperature ≈ 0.1 K above the zero-field transition temperature. Lattice strain—the parameter analogous to the tilt angle—and polarization of KDP in an external field show qualitatively the same dependence on field strength and temperature as reported in this paper for the C7 ferroelectric liquid crystal.

Phase transitions in liquid crystals are strongly dependent on the composition of the system. Recently it was shown[21] that, by adding a second liquid-crystal compound, the first-order Sm-*A*–Sm-*C* transition of the C7 liquid crystal can be driven towards second-order crossing a tricritical point in the transition line in the temperature-composition plane. We have studied the influence of an electric field on the second-order Sm-*A*–Sm-*C* transition of such a mixture (C7+10.0.4, see experimental section) by measurements of tilt angle and dielectric constant in the presence of a dc electric field. Figure 8 shows the electric field dependence of the tilt angle at various temperatures near the Sm-*A*–Sm-*C* transition of the mixture. As expected and shown recently by other groups,[22,23] the θ-E curves are linear for temperatures far above the transition (curve *a*) whereas they deviate from the linear shape and show a negative curvature when the transition temperature is approached (curves *b*–*e*). Below the transition temperature, the θ-E curves lead to a nonzero θ for $E=0$ and the curvature becomes weaker when the temperature is decreased further (curves *f*–*j*). In contrast to the behavior at the first-order Sm-*A*–Sm-*C* transition (Fig. 4) the θ-E curves do not show an S-like shape or a discontinuity, i.e., a phase transition exists only for zero external field if the Sm-*A*–Sm-*C* transition is second order.[24] Accordingly, the dielectric constant varies continuously with temperature when a dc bias field is applied (Fig. 9): the maximum of the dielectric constant obtained at the low bias field of 1.7 kV/cm (curve *a*) is rapidly decreased by slight increases of the bias field, at 11.9 kV/cm (curve *g*) only a weak enhancement of the dielectric constant in the temperature region of the second-order transition is observable. We should note that a bias field, in contrast to the situation at the first-order transition, causes always a decrease of the susceptibility values in the whole temperature range according to the fact that the θ versus E curves exhibit only negative curvature. This behavior might be used to distinguish a second-order transition from a weak first-order transition where, in a certain temperature range, a slight increase of the susceptibility values by a bias field is observable.[25]

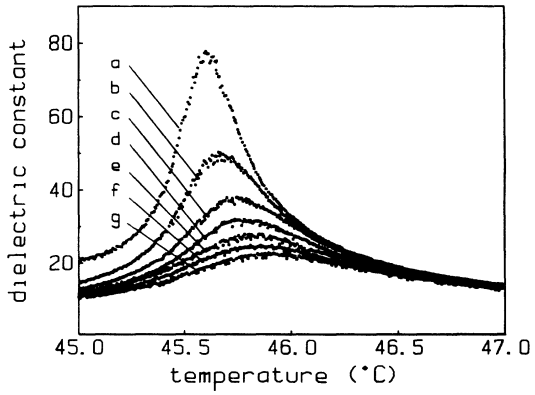

FIG. 9. Temperature dependence of the static dielectric constant of the second-order mixture at various bias fields. The values of the bias field are (in kV/cm) curve *a*, 1.7; curve *b*, 3.4; curve *c*, 5.1; curve *d*, 6.8; curve *e*, 8.5; curve *f*, 10.2; curve *g*, 11.9.

IV. LANDAU DESCRIPTION

The experimental behavior and the critical point described above can be interpreted by a simple Landau model. For an improper ferroelectric with a linear coupling between polarization and order parameter we can write down the following equation for the Landau free-energy density:[26]

$$g=g_0+\tfrac{1}{2}a(T-T_0)\theta^2+\tfrac{1}{4}b\theta^4+\tfrac{1}{6}c\theta^6+\frac{1}{2\chi_0\epsilon_0}P^2-CP\theta-EP \quad (1)$$

with θ denoting the tilt angle, P the polarization, E the electric field strength, ϵ_0 the vacuum permittivity, χ_0 the susceptibility at fixed tilt angle (i.e., without contributions of the P-θ coupling), and C the bilinear tilt-polarization coupling constant. T_0 is the temperature of the stability limit of the high-temperature phase for the system with $C=0$ and $E=0$. With $a,c>0$ and $b<0$ this equation describes a first-order transition and a linear coupling between polarization and tilt angle ($P=\chi_0\epsilon_0 C\theta+\chi_0\epsilon_0 E$). The last term, $-EP$, gives the energy decrease by the external electric field. Because the critical point we want to describe is due to a linear coupling to the field, we neglect here any higher-order terms in E.

Recent Landau theories[27,28] of ferroelectric liquid crystals include several additional terms describing the complex temperature dependence of the P/θ ratio and the helical pitch in the Sm-C phase. Especially a biquadratic $P^2\theta^2$ coupling term[29] is necessary to give an exact description of the temperature dependence of P_s. However, since we have shown in an earlier study[30] that the ferroelectric properties of high polarization compounds such as C7 can be described to a good approximation taking into account only the linear $P\theta$ coupling term (i.e., in high polarization compounds the biquadratic term is small compared to the bilinear term), we have neglected here the biquadratic coupling. Also we have neglected the helical superstructure of the Sm-C phase because the critical point to be described occurs at a field strength far above the unwinding field.

The stable state of the system is defined by the minimum of the free energy with respect to the order parameter tilt angle. Setting $\partial g/\partial\theta=0$, we can derive an equation for the electric field strength as a function of temperature and tilt angle:

$$E=\frac{1}{C\chi_0\epsilon_0}\{[a(T-T_0)-C^2\chi_0\epsilon_0]\theta+b\theta^3+c\theta^5\} . \quad (2)$$

The family of curves defined by Eq. (2) is shown in Fig. 10 for $b<0$ (first-order transition) and $b>0$ (second-order transition). In the first-order case, the θ-E curves are S-like in shape, corresponding to a discontinuous transition, if the temperature is close to T_{c_0}. The first-order transition vanishes at a critical temperature T_c, at which the θ-E curve exhibits a vertical inflection point. On increasing the temperature further, the θ-E curves approach the usual linear electroclinic behavior of the Sm-A phase. At the critical point the equations $\partial E/\partial\theta=0$ and $\partial^2 E/\partial\theta^2=0$ must be satisfied and we can derive expressions for the critical tilt angle θ_c, the critical temperature T_c, and the critical field E_c:[31]

$$\theta_c=(-3b/10c)^{1/2} , \quad (3)$$

$$T_c=T_0+\frac{9b^2}{20ac}+\frac{C^2\chi_0\epsilon_0}{a} , \quad (4)$$

$$E_c=\frac{1}{C\chi_0\epsilon_0}\left[\frac{6\sqrt{3}}{25\sqrt{10}}\frac{(-b)^{5/2}}{c^{3/2}}\right] . \quad (5)$$

Since the transition temperature for zero field is given by $T_{c_0}=T_0+3b^2/(16ac)+C^2\chi_0\epsilon_0/a$, we get, for the difference $T_c-T_{c_0}$,

$$T_c-T_{c_0}=21b^2/(80ac) . \quad (6)$$

The theoretical θ-E curves shown in Fig. 10 appear very similar to our experimental results for the first-order (Figs. 4 and 5) as well as for the second-order system (Fig. 8) and for the first-order case we tried a quantitative fit of the Landau free-energy parameters. The value of the

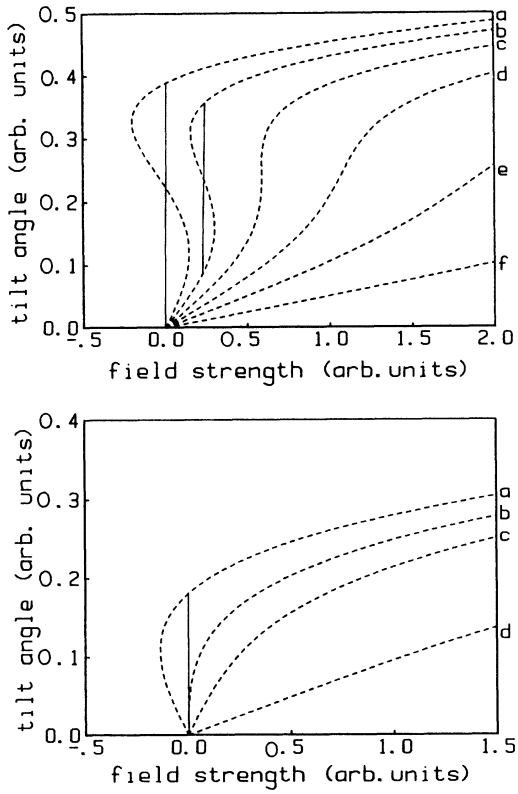

FIG. 10. Theoretically tilt angle vs field strength curves (dashed lines) according to Eq. (2) (vertical solid lines indicate discontinuous transitions). Above: first-order transition ($b<0$), curve a: $T=T_{c_0}$; curve b: $T_{c_0}<T<T_c$; curve c: $T=T_c$; curve d: $T>T_c$; curves e, f: $T\gg T_c$ (T_{c_0} denotes the zero-field first-order transition temperature and T_c the critical-point temperature). Below: second-order transition ($b>0$), curve a: $T<T_c$; curve b: $T=T_c$; curve c: $T>T_c$; curve d: $T\gg T_c$ (T_c denotes here the second-order transition temperature).

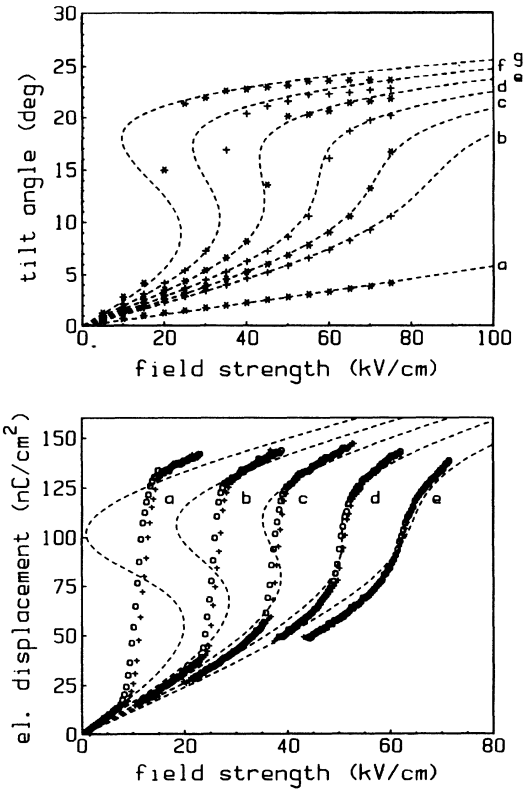

FIG. 11. Comparison between experimental data and theoretical curves (dashed lines) for C7. The tilt-angle values (above) are calculated according to Eq. (2) using the parameter values given in Table I [differences to T_{c_0} (in K): curve *a*, +3.1; curve *b*, +1.3; curve *c*, +1.1; curve *d*, +0.9; curve *e*, +0.7; curve *f*, +0.5; curve *g*, +0.3]. The theoretical values of the electric displacement (below) are calculated from the theoretical tilt-angle values according to $D=P+\epsilon_0 E$ with $P=\chi_0\epsilon_0(C\theta+E)$. Temperature differences to T_{c_0} (in K): curve *a*, +0.2; curve *b*, +0.4; curve *c*, +0.6; curve *d*, +0.8; curve *e*, +1.0.

tilt-polarization coupling constant C can be measured as the ratio between electric susceptibility and tilt susceptibility as described in Refs. 32 and 33. For the susceptibility at fixed tilt angle χ_0 we took the value of the racemic version of a compound very similar to C7.[32] The amounts of the parameters *a*, *b*, and *c* are then chosen to give a maximum agreement between theory and experiment. Although there are slight discrepancies at high fields and large tilt-angle values, we can achieve a very good overall agreement (Fig. 11) between theoretical and experimental tilt-angle data using the parameter values given in Table I. Remarkably, with the same set of parameters our polarization data are described with almost

TABLE I. Values of the Landau free-energy parameters.

a	8.93×10^4 J m^{-3} K^{-1} rad^{-2}
b	-1.34×10^6 J m^{-3} rad^{-4}
c	6.57×10^6 J m^{-3} rad^{-6}
T_0	51.36 °C
χ_0	4.2
C	8.58×10^7 J C^{-1} m^{-1} rad^{-1}

the same agreement between theoretical and experimental values, indicating that a simple bilinear tilt-angle–polarization coupling is sufficient to describe, to a good approximation, the behavior of our sample (Fig. 11). Calculating the critical-point coordinates using Eqs. (3)–(6) we get the following values which are well in agreement with our estimations of the corresponding experimental values: $\theta_c=14.2°$, $T_c-T_{c_0}=0.76$ K, and $E_c=50.7$ kV/cm. Calculating the value of the electric displacement at the critical point according to $D_c=C\chi_0\epsilon_0\theta_c+(\chi_0+1)\epsilon_0 E_c$ we find $D_c=102$ nC/cm^2 again coinciding well with our experimental observation.

V. CONCLUSION

Our measurements of tilt angle, polarization, and susceptibility of a ferroelectric liquid crystal with a first-order Sm-A–Sm-C transition establish the existence of a line of first-order transitions in the temperature-field plane terminating at a critical point. The first-order transition in the presence of a dc electric field is characterized by a discontinuity of tilt angle, polarization, and susceptibility. At the critical point the discontinuity of tilt angle and polarization vanishes and the susceptibility exhibits a divergencelike behavior. Measurements of tilt angle and susceptibility of a similar liquid-crystal system with a second-order Sm-A–Sm-C transition have clearly demonstrated the different behavior of first-order and second-order samples in an external electric field.

The experimental behavior of the ferroelectric liquid crystal is very similar to the solid-state ferroelectric crystal KDP. For KDP it was argued[34] that there are no microscopic fluctuations at the paraelectric-ferroelectric critical point. The fact that the overall behavior of the ferroelectric liquid crystal can be described quantitatively by a simple Landau model might indicate a similar situation for the liquid crystal. Clearly, further studies, especially in the immediate vicinity of the critical point, are needed to clarify the nature of this new critical point in liquid-crystal phase transitions.

Another aspect for further investigations concerns the tricritical behavior of the Sm-A–Sm-C transition. In the temperature-field-concentration space the critical point described here belongs to two lines (for positive and for negative field) of critical points which end at a tricritical point where they join with the second-order Sm-A–Sm-C transition line lying in the temperature-concentration plane (with zero external field). Thus the two ferroelectric liquid-crystal samples described here belong to a system where all the three lines of critical points defining a tricritical point[35] are experimentally accessible. This is not the case in most other physical systems exhibiting tricritical behavior (e.g., He^3-He^4 mixtures, metamagnetic-antiferromagnetic compounds, nematic–smetic-A liquid crystals), because the field conjugated to the order parameter is not experimentally available. Thus, experimental studies of the polarized Sm-A–ferroelectric-Sm-C critical point may be of interest also in the vicinity of a Sm-A–Sm-C tricritical point.

ACKNOWLEDGMENTS

This work was supported by the Deutsche Forschungsgemeinschaft (Sonderforschungsbereich 335). We would like to thank J. Prost for stimulating discussions and J. Fousek for drawing our attention to the ferroelectric compound KDP.

[1]For recent reviews on ferroelectric liquid crystals see R. Blinc, C. Filipic, A. Levstik, B. Zeks, and T. Carlsson, Mol. Cryst. Liq. Cryst. **151**, 1 (1987); S. T. Lagerwall, B. Otterholm, and K. Skarp, *ibid.* **152**, 503 (1987); L. A. Beresnev, L. M. Blinov, M. A. Osipov, and S. A. Pikin, *ibid.* **158A**, 3 (1988).

[2]R. B. Meyer, L. Liebert, L. Strzelecki, and P. Keller, J. Phys. (Paris) Lett. **36**, L69 (1975).

[3]S. Garoff and R. B. Meyer, Phys. Rev. Lett. **38**, 848 (1977); Phys. Rev. A **19**, 338 (1979).

[4]P. G. de Gennes, Mol. Cryst. Liq. Cryst. **21**, 49 (1973).

[5]C. A. Schantz and D. L. Johnson, Phys. Rev. A **17**, 1504 (1978).

[6]C. R. Safinya, M. Kaplan, J. Als-Nielsen, R. J. Birgeneau, D. Davidov, J. D. Litster, D. L. Johnson, and M. E. Neubert, Phys. Rev. B **21**, 4149 (1980).

[7]C. C. Huang and J. M. Viner, Phys. Rev. A **25**, 3385 (1982).

[8]R. J. Birgeneau, C. W. Garland, A. R. Kortan, J. D. Litster, M. Meichle, B. M. Ocko, C. Rosenblatt, L. J. Yu, and J. W. Goodby, Phys. Rev. A **27**, 1251 (1983); M. Meichle and C. W. Garland, Phys. Rev. A **27**, 2624 (1983).

[9]B. M. Ocko, A. R. Kortan, R. J. Birgeneau, and J. W. Goodby, J. Phys. (Paris) **45**, 113 (1984).

[10]S. C. Lien, C. C. Huang, and J. W. Goodby, Phys. Rev. A **29**, 1371 (1984).

[11]S. C. Lien and C. C. Huang, Phys. Rev. A **30**, 624 (1984).

[12]S. Dumrongrattana, C. C. Huang, G. Nounesis, S. C. Lien, and J. M. Viner, Phys. Rev. A **34**, 5010 (1986).

[13]Ch. Bahr and G. Heppke, Mol. Cryst. Liq. Cryst. **148**, 29 (1987); B. R. Ratna, R. Shashidhar, Geetha G. Nair, S. Krishna Prasad, Ch. Bahr, and G. Heppke, Phys. Rev. A **37**, 1824 (1988).

[14]R. B. Meyer, Mol. Cryst. Liq. Cryst. **40**, 33 (1977).

[15]H. Y. Liu, C. C. Huang, Ch. Bahr, and G. Heppke, Phys. Rev. Lett. **61**, 345 (1988); G. Heppke, D. Lötzsch, and R. Shashidhar, Liq. Cryst. **5**, 489 (1989); H. Y. Liu, C. C. Huang, T. Min, M. D. Wand, D. M. Walba, N. A. Clark, Ch. Bahr, and G. Heppke, Phys. Rev. A **40**, 6759 (1989).

[16]Ch. Bahr and G. Heppke, Phys. Rev. A **39**, 5459 (1989).

[17]T. P. Rieker, N. A. Clark, G. S. Smith, D. S. Parmar, E. B. Sirota, and C. R. Safinya, Phys. Rev. Lett. **59**, 2658 (1987).

[18]W. J. Merz, J. Appl. Phys. **27**, 938 (1956); Ph. Martinot-Lagarde, J. Phys. (Paris) Lett. **38**, L17 (1977).

[19]J. Kobayashi, Y. Uesu, and Y. Enomoto, Phys. Status Solidi B **45**, 293 (1971).

[20]A. B. Western, A. G. Baker, C. R. Bacon, V. H. Schmidt, Phys. Rev. B **17**, 4461 (1978), and references therein.

[21]R. Shashidhar, B. R. Ratna, Geetha G. Nair, S. Krishna Prasad, Ch. Bahr, and G. Heppke, Phys. Rev. Lett. **61**, 547 (1988).

[22]S. Nishiyama, Y. Ouchi, H. Takezoe, and A. Fukuda, Jpn. J. Appl. Phys. **26**, L1787 (1987).

[23]Sin-Doo Lee and J. S. Patel, Appl. Phys. Lett. **54**, 1653 (1989).

[24]The only transition which can be observed for a second-order sample in the presence of a dc electric field is the transition from the unwound homogeneous polarized state to a state with a distorted helical structure at lower temperature; see, e.g., S. Dumrongrattana and C. C. Huang, J. Phys. (Paris) **47**, 2117 (1986), and references therein.

[25]Ch. Bahr, G. Heppke, and N. K. Sarma, Ferroelectrics **76**, 151 (1987).

[26]M. E. Lines and A. M. Glass, *Principles and Applications of Ferroelectrics and Related Materials* (Clarendon, Oxford, 1979), pp. 353–355.

[27]C. C. Huang and S. Dumrongrattana, Phys. Rev. A **34**, 5020 (1986).

[28]T. Carlsson, B. Zeks, A. Levstik, C. Filipic, I. Levstik, and R. Blinc, Phys. Rev. A **36**, 1484 (1987).

[29]B. Zeks, Mol. Cryst. Liq. Cryst. **114**, 259 (1984).

[30]Ch. Bahr, G. Heppke, and B. Sabaschus, Ferroelectrics **84**, 103 (1988).

[31]Similar calculations were carried out for the solid-state ferroelectrics KDP, see Refs. 19 and 20, and $BaTiO_3$, see W. J. Merz, Phys. Rev. **91**, 513 (1953).

[32]Ch. Bahr and G. Heppke, Liq. Cryst. **2**, 825 (1987).

[33]Ch. Bahr and G. Heppke, Phys. Rev. A **37**, 3179 (1988).

[34]E. Courtens, R. Gammon, and S. Alexander, Phys. Rev. Lett. **43**, 1026 (1979).

[35]R. B. Griffiths, Phys. Rev. Lett. **24**, 715 (1970).